
**OPTICAL-PHYSICAL METHODS
OF RESEARCH AND MEASUREMENT**

Photorefractive Changes in the Refractive Index in a LiNbO₃:Cu Crystal with a Surface Doping

A. D. Bezpaly^{1*}, V. I. Bykov¹, and A. E. Mandel¹

¹Tomsk State University of Control Systems and Radioelectronics, Tomsk, 634050 Russia

Received February 11, 2022; revised March 11, 2022; accepted March 11, 2022

Abstract—Changes in the refractive index induced in the Cu-doped surface layer of a lithium niobate crystal were investigated experimentally. The changes were induced by sequential point-by-point exposure of an experimental sample by focused laser radiation at a wavelength of $\lambda = 532$ nm.

DOI: 10.3103/S8756699022020017

Keywords: *optical induction, refractive index change, lithium niobate, surface layer, Jamin interferometer*

1. INTRODUCTION

The creation and development of devices for data retrieval, processing, and transmission on the basis of integrated optics and waveguide photonics have attracted the interest of many researchers [1–5]. Elements of localization and conversion of light signals, such as waveguide and diffraction structures, are of particular importance in integrated optics devices. Lithium niobate crystal (LiNbO₃) is widely used for the implementation of various photonic devices on the basis of these structures [2–4, 6]. Bulk or surface doping of LiNbO₃ crystals with various impurities, such as iron (Fe), copper (Cu), titanium (Ti), and manganese (Mn), changes the optical and photorefractive properties of crystals [2, 7–9]. Unlike bulk doping, surface doping of LiNbO₃ makes it possible to use different concentrations of impurity ions in the material structure in various parts of the same substrate. This makes it possible to implement waveguide and diffractive structures with individual characteristics as well as complex topologies of integrated optical circuits [2, 7, 10].

Due to the photorefractive effect in LiNbO₃ crystals, the integrated optical structures can be formed by laser radiation [2, 6, 10–13]. Laser-radiation-induced changes in the refractive index in bulk-doped samples of LiNbO₃ and samples without impurities were addressed in [14–16].

The study [14] considered a bulk-doped *Y*-cut LiNbO₃:Fe crystal using a Mach–Zehnder interferometer. The crystalline sample was irradiated with a collimated laser beam ($\lambda = 532$ nm) with a diameter of 0.2 mm and a power density of 60 mW/cm². The authors of [14] also showed that the induced changes in the refractive index along the optical axis of the crystal have an alternating character. The level of negative changes in the refractive index after irradiation of the crystal reached $\Delta n_o = -16 \times 10^{-4}$ in 60 s and the level of positive changes reached $\Delta n_o = 8 \times 10^{-4}$. In [15], the changes in the refractive index were induced in an undoped LiNbO₃ crystal by an inhomogeneous light field generated by a Michelson interferometer. The polarization of radiation in the experiments corresponded to ordinary and extraordinary waves of the crystal. The CCD camera recorded the shift of the interference pattern during laser radiation exposure. The induced changes in the refractive index in the crystal reached the saturation level $\Delta n_o = 1,2 \times 10^{-4}$ for an ordinary wave and $\Delta n_e = 6,6 \times 10^{-4}$ for an extraordinary wave. Paper [16] investigated the influence of thermal effects on induced changes in the refractive index in LiNbO₃:Fe crystals under continuous local irradiation of experimental samples with argon laser radiation ($\lambda = 515$ nm). The light spot diameter was 130 μ m and the laser power density

*E-mail: aleksandr.bezpalyi@tusur.ru

varied from 75 to 9000 W/cm². The influence of temperature on the induced changes in the refractive index Δn was observed when the sample was illuminated for several minutes with radiation of a power density of around 450 W/cm² or more. The experiments on the illumination of samples by radiation with a power density of 75 W/cm² showed that the changes in the extraordinary refractive index are negative and reach $\Delta n_e = -6 \times 10^{-4}$. As the radiation power density increased to 9000 W/cm², the changes in the extraordinary refractive index became positive and amounted to $\Delta n_e = 7 \times 10^{-4}$. This is explained by the fact that at a high power density during local illumination, the sample heats up and the inhomogeneous temperature change amplifies the spatially modulated positive pyroelectric field, which is compensated after the illumination is turned off by the negative field of the spatial charge.

The changes in the refractive index in LiNbO₃ crystals can be optically induced in various ways, such as using an amplitude mask [10] or focusing laser radiation with a cylindrical lens [17]. According to [17–19], optical induction of waveguide structures in doped LiNbO₃ crystals can be performed by sequential point-by-point exposure by a spherical lens, forming a light beam on the crystal surface, which makes it possible to specify the topology and spatial dimensions of waveguide structures during their formation as well as to control the localization of laser radiation over the depth of the crystal [17–20].

This paper aims to experimentally investigate the changes in the refractive index induced point-by-point by focused laser radiation in the surface layer of a Cu-doped LiNbO₃ crystal.

2. CHANGES INDUCED BY LASER RADIATION IN A SURFACE-DOPED LiNbO₃ CRYSTAL

The experiments used an *X*-cut lithium niobate crystal with dimensions of 1.25 × 10 × 14 mm along the *X*, *Y*, and *Z* axes, respectively. The surface layer of the crystal was doped with copper ions. The average concentration of ions in the crystal surface layer was $C_{Cu} \approx 16.8 \times 10^{24} \text{ m}^{-3}$ [21]. The depth of the doped layer along the *X*-axis of the crystal was measured by laser beam probing ($\lambda = 633 \text{ nm}$) according to the technique described in [20]. The experimentally measured normalized dependence of the absorption coefficient α on the coordinate *X* of the crystal is shown in Fig. 1. It can be seen from the graph that the largest part of the doping impurity is contained in the crystal surface layer with a thickness of $h \approx 300 \mu\text{m}$.

Point-by-point formation of structures in the doped layer of the LiNbO₃ crystal was performed using a solid-state YAG:Nd³⁺ laser operating in the continuous mode with frequency doubling ($\lambda = 532 \text{ nm}$) as a radiation source. The experimental sample was placed on a micrometer positioner with a shift accuracy of 5 μm . The light beam was focused on the sample surface by a microobjective (Fig. 2a). The light beam diameter was $\sim 50 \mu\text{m}$ at the level of 0.1 maximum intensity. The polarization of laser radiation corresponded to the extraordinary wave of the crystal. The power density of the light wave was $\sim 500 \text{ W/cm}^2$. In different experiments, the exposure time of the surface layer by a single focused light spot varied from 2 to 60 s. Induction of a set of points allows for the creation of regions in the form of strips along the *Y*-axis of a crystal with a changed refractive index (Fig. 2b). Each strip consisted of 40 dots located 25 μm away from each other.

Changes in the refractive index in the structures induced in the surface layer of LiNbO₃ were investigated by analyzing the interference patterns formed by the Jamin interferometer. The sample was placed in one of the arms of the interferometer. This analysis makes it possible to determine the spatial profile of induced changes in the refractive index even if the size of the inducing light spot is small [22].

The schematic of the experimental setup for studying the changes induced in the sample is shown in Fig. 3a. The radiation source was a He–Ne laser ($\lambda = 633 \text{ nm}$) with light wave polarization parallel to the optical axis of the crystal and output power of $\sim 1 \text{ mW}$. The structures under study were probed with collimated laser radiation directed to beam-splitting element 2, which splits the radiation into two light beams. Sample 3 was placed with induced structures in one of the arms of the interferometer. The second mirror 4 of the interferometer combined light beams, forming interference patterns, which were projected by spherical lens 5 onto the matrix of CCD camera 6 connected to computer 7. Examples of the resulting interferograms for 5- and 60-s exposures of the sample surface are shown in Figs. 3b and 3c. The regions of induced changes in the refractive index are marked with a dashed line.

The magnitude and nature of the induced changes in the refractive index in the crystal were investigated by processing the obtained interferograms using the technique described in [14, 15, 23].

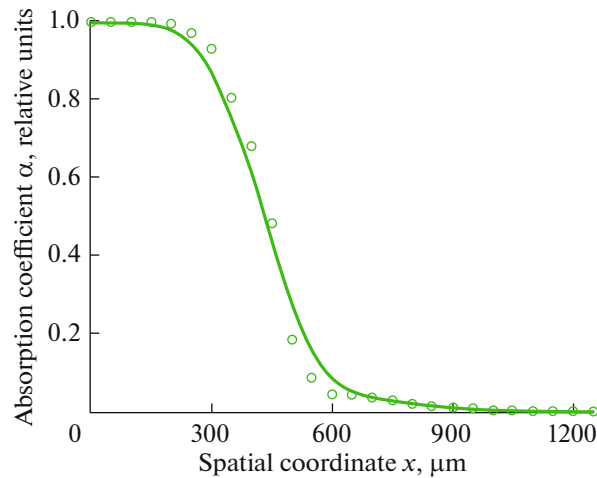


Fig. 1. Absorption coefficient as a function of doping depth of the crystal.

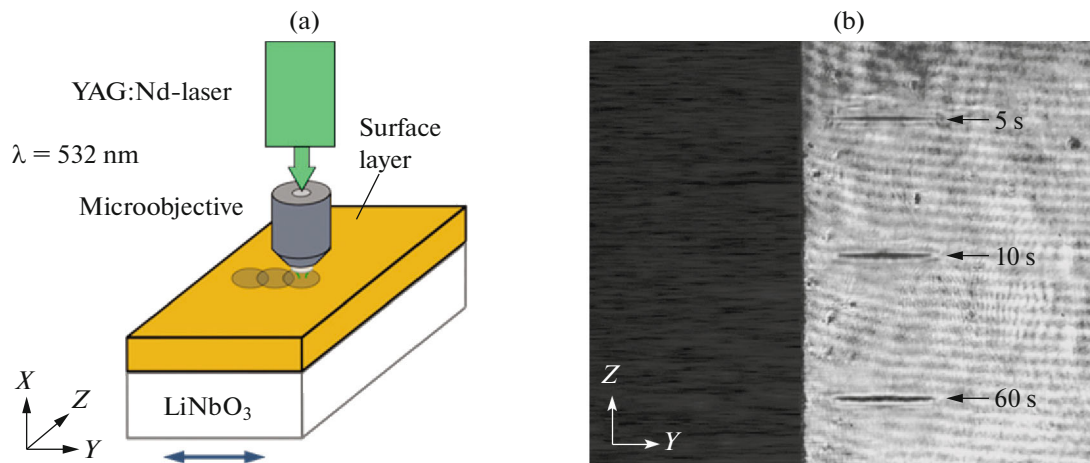


Fig. 2. Point-by-point induction of changes in the refractive index in the surface layer of a $\text{LiNbO}_3\text{:Cu}$ crystal: (a) schematic of the induction process and (b) light pattern on the output face of the crystal, obtained by probing of point-by-point induced regions.

Figure 4 shows an example of the reconstructed phase front of a light wave passing through the region of induced changes. The phases were determined after filtering the spectrum obtained by a Fourier transform of original interferograms. The interferograms before and after exposure of the crystal by laser radiation are shown in Figs. 4a and 4b. The inverse Fourier transform makes it possible to reconstruct the folded phase pattern with the removed phase component (Figs. 4c and 4d). However, the discontinuities in the folded phase patterns do not allow the wave front in the region of induced changes to be accurately reconstructed (Fig. 4e). These discontinuities can be eliminated by unfolding the phases. Subtraction of patterns with a continuous phase distribution before and after laser-induced changes makes it possible to reconstruct the phase front in the region of induced changes in the refractive index (Fig. 4f). The interferogram shown in Fig. 4b was obtained with a 5-s exposure of a single point of the induced strip.

Reconstruction of the wavefront of a light wave passing through the induced structure makes it possible to estimate the magnitude and distribution of induced changes in the refractive index. The changes in the refractive index Δn_e along the Z -axis of the crystal at different exposure times can be determined by the formula [13–16]

$$\Delta n(z) = \frac{\lambda \Delta \varphi(z)}{2\pi d_x}, \quad (1)$$

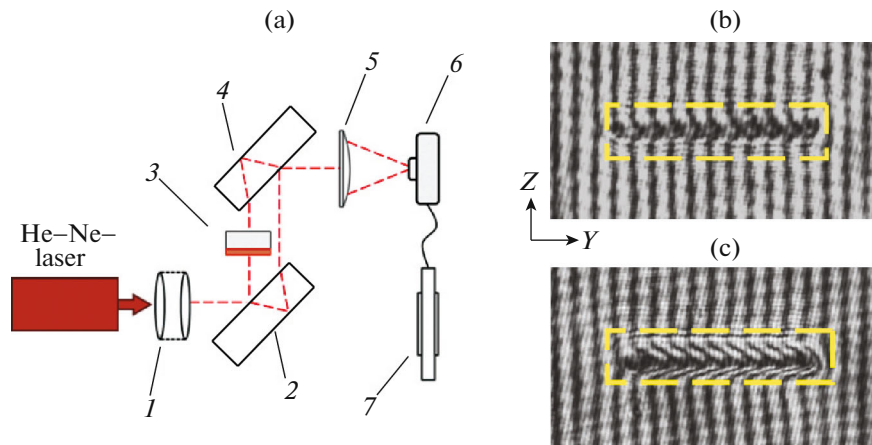


Fig. 3. Induced changes in the refractive index in the surface layer of a LiNbO₃ crystal: (a) schematic of the experimental setup based on a Jamin interferometer; (b) interference pattern in the region of changes induced during a 5-s exposure of a single point in the strip; and (c) interference pattern in the region of changes induced during a 60-s exposure of a single point in the strip.

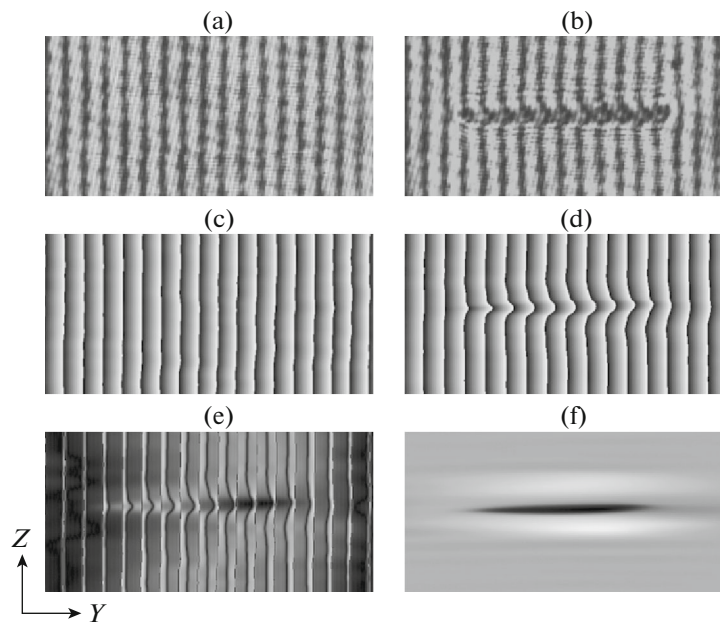


Fig. 4. Stages of visualization of induced changes in the refractive index in a surface-doped LiNbO₃:Cu crystal with a 5-s exposure of a single point: (a) interferogram before crystal exposure; (b) interferogram after crystal exposure; (c) folded phase obtained from interferogram (a); (d) folded phase obtained from interferogram (b); (e) difference between folded phases (c) and (d); and (f) phase front of the wave passing through the region of induced changes.

where λ is the wavelength of radiation in the interferometer; $\Delta\varphi(z)$ is the phase shift, and d_x is the depth of induced changes in the refractive index along the X -axis of the crystal.

In formula (1), the phase shift $\Delta\varphi(z)$ of interference strips induced by the region with a changed refractive index was averaged over the entire length of the induced strip. The depth of induced changes d_x along the X -axis of the crystal were determined through additional studies. Regions with a changed refractive index in the form of strips with a length of $\sim 750 \mu\text{m}$ were formed near the end of the crystal by point-by-point exposure by light with a wavelength of 532 nm. Each strip consisted of 30 dots located $25 \mu\text{m}$ away from each other. The exposure time of the crystal with a single focused light spot varied from 2 to 60 s.

A typical example of interferograms from the end surface of the sample (XZ -plane), obtained by

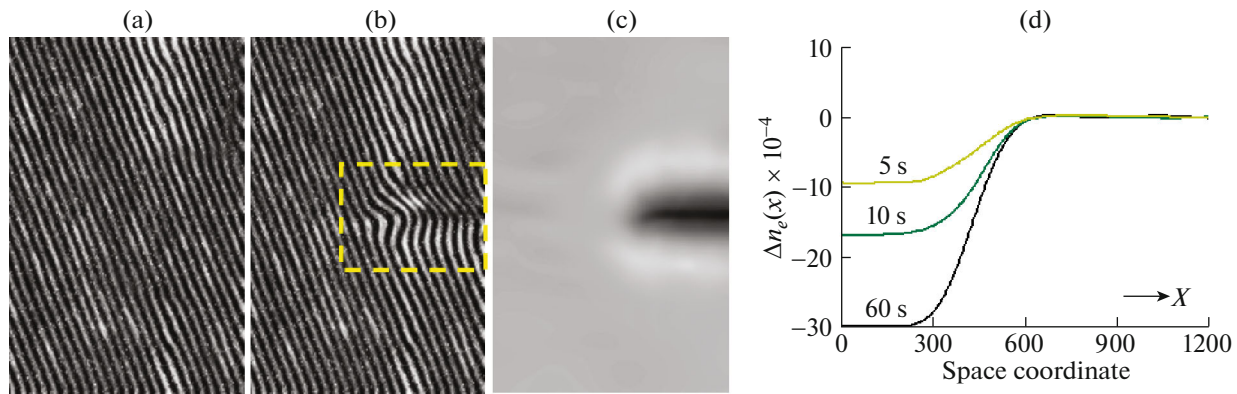


Fig. 5. Interferogram at the end of the crystal: (a) before exposure of the YZ -surface; (b) in the region of the exposed strip (with a 5-s exposure by one spot); (c) reconstructed phase front in the region of the induced strip; (d) induced changes in refractive index Δn_e along the X -axis of the crystal.

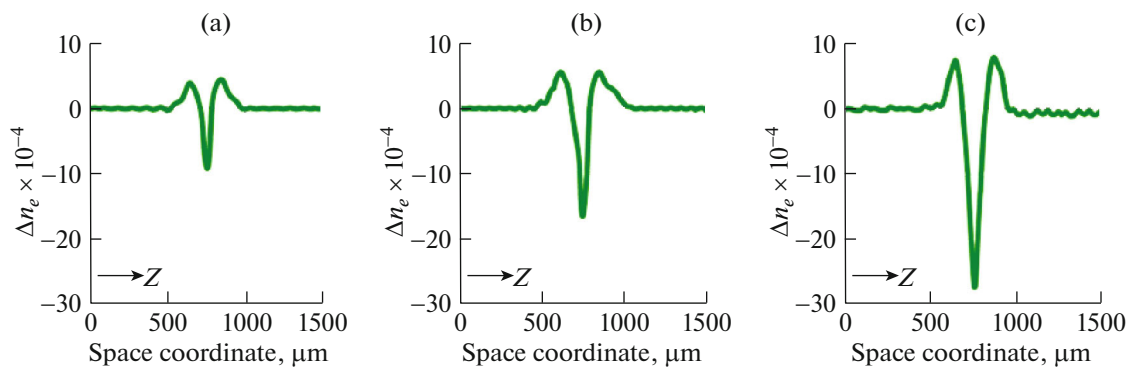


Fig. 6. Induced changes in refractive index along the optical axis of the $\text{LiNbO}_3\text{:Cu}$ crystal at a time of exposure by a single spot: (a) 5; (b) 10; (c) 60 s.

placing the crystal in one of the arms of the Jamin interferometer before and after induced changes is shown in Figs. 5a, 5b. An example of the reconstructed phase front is shown in Fig. 5c. The induced changes in the refractive index Δn_e along the X -axis of the crystal, obtained in this experiment at different exposure times are shown in Fig. 5d. The maximum induced changes in the refractive index occur in the doped layer of the crystal with a thickness of $d_x = 300 \mu\text{m}$. At a depth of $600 \mu\text{m}$, there are almost no changes in the refractive index induced in the crystal.

The changes in the refractive index Δn_e of the surface layer along the Z -axis at different exposure times were calculated taking into account the depth of induced changes in the refractive index along the X -axis of the crystal. The induced changes in the refractive index along the optical axis of the $\text{LiNbO}_3\text{:Cu}$ crystal, averaged over the entire length of the strip with a changed refractive index and at different exposure times for a single spot are shown in Fig. 6.

It can be seen from the above presented graphs that the changes in the refractive index along the optical axis of the crystal have the following character: a dip with a negative change in the refractive index is generated in the center of the illuminated area and hills with a positive change are generated at its edges.

In the experiments with point-by-point exposure of a $\text{LiNbO}_3\text{:Cu}$ crystal, the negative and positive changes in the refractive index reach the saturation level $\Delta n_e = -28 \times 10^{-4}$ and $\Delta n_e = 7,5 \times 10^{-4}$ within 40 s. With an increase in the illumination time to 60 s, the level of changes in the refractive index remains almost unchanged.

Exposure of the surface-doped $\text{LiNbO}_3\text{:Cu}$ crystal by focused laser radiation leads to significant changes in the refractive index in the illuminated region inside the surface layer. Since the power density in the experiments did not exceed 500 W/cm^2 , the contribution of temperature effects to the change

in the refractive index can be neglected [16]. The main contribution to the induced changes Δn of the sample is due to the photorefractive effect. The estimate for the space charge field E_{sc} based on the experimentally obtained values of induced changes Δn varies from 3×10^4 to 2×10^5 V/cm (at different exposure times). The magnitude of the space charge field E_{sc} coincides with the calculated values given in [8, 24, 25].

3. CONCLUSIONS

Changes in the refractive index induced by focused laser radiation in the surface layer of a LiNbO₃ crystal have been experimentally investigated. When the crystal was exposed by continuous radiation with $\lambda = 532$ nm and extraordinary polarization, the peak negative changes reach $\Delta n_e = -28 \times 10^{-4}$. It has been shown that the magnitude of the induced changes in the refractive index can be controlled by changing the crystal exposure time. The spatial profile of induced changes in the locally illuminated area has an alternating character. The results obtained in this paper can be used in modeling and designing integrated optical circuits, hybrid and all-optical devices.

FUNDING

This study was supported by the “Priority 2030” Strategic Academic Leadership Program, project no. Pr2030-Nauka SCh/SP1/B/8.

CONFLICT OF INTEREST

The authors declare that they have no conflicts of interest.

REFERENCES

1. B. C. Hitz, J. J. Ewing, and J. Hecht, *Introduction to Laser Technology*, 4th ed. (John Wiley & Sons, Hoboken, N.J., 2012).
2. M. Bazzan and C. Sada, “Optical waveguides in lithium niobate: Recent developments and applications,” *Appl. Phys. Rev.* **2**, 040603 (2015). <https://doi.org/10.1063/1.4931601>
3. D. Pohl, A. Messner, F. Kaufmann, M. R. Escalé, J. Holzer, J. Leuthold, and R. Grange, “100-GBd waveguide bragg grating modulator in thin-film lithium niobate,” *IEEE Photonics Technol. Lett.* **33**, 85–88 (2021). <https://doi.org/10.1109/LPT.2020.3044648>
4. G. Chen, H.-L. Lin, J. D. Ng, and A. J. Danner, “Integrated thermally tuned Mach–Zehnder interferometer in Z-Cut lithium niobate thin film,” *IEEE Photonics Technol. Lett.* **33**, 664–667 (2021). <https://doi.org/10.1109/LPT.2021.3086850>
5. Yu. Jia and F. Chen, “Compact solid-state waveguide lasers operating in the pulsed regime: A review,” *Chin. Opt. Lett.* **17**, 012302 (2019).
6. B. Zhang, L. Li, B. Wu, H. Liu, P. Wu, L. Wang, and F. Chen, “Femtosecond laser inscribed novel polarization beam splitters based on tailored waveguide configurations,” *J. Lightwave Technol.* **39**, 1438–1443 (2021).
7. C. Pang, R. Li, Z. Li, N. Dong, F. Ren, J. Wang, and F. Chen, “A novel hierarchical nanostructure for enhanced optical nonlinearity based on scattering mechanism,” *Small* **16**, 2003172 (2020). <https://doi.org/10.1002/sml.202003172>
8. M. P. Petrov, S. I. Stepanov, and A. V. Khomenko, *Photorefractive Crystals in Coherent Optics* (Nauka, St. Petersburg, 1992).
9. K. K. Wong, *Properties of Lithium Niobate* (INPSEC, The Institution of Electrical Engineers, London, 2002).
10. S. A. Davydov, P. A. Trenikhin, V. M. Shandarov, K. V. Shandarova, D. Kip, Ch. Ruter, and F. Chen, “Quasione-dimensional photonic lattices and superlattices in lithium niobate: Linear and nonlinear discrete diffraction of light,” *Phys. Wave Phenom.* **18**, 1–6 (2010). <https://doi.org/10.3103/S1541308X10010012>
11. L. Vittadello, A. Zaltron, N. Argiolas, M. Bazzan, N. Rossetto, and R. Signorini, “Photorefractive direct laser writing,” *J. Phys. D: Appl. Phys.* **49**, 125103 (2016). <https://doi.org/10.1088/0022-3727/49/12/125103>
12. Q. Zhang, M. Li, J. Xu, Z. Lin, H. Yu, M. Wang, Z. Fang, Ya Cheng, Q. Gong, and Y. Li, “Reconfigurable directional coupler in lithium niobate crystal fabricated by three-dimensional femtosecond laser focal field engineering,” *Photonics Res.* **7**, 503–507 (2019). <https://doi.org/10.1364/PRJ.7.000503>

13. N. Tarjanyi and D. Kacik, "Lithium niobate-based integrated photonics utilizing photorefractive effect," *Commun. Sci. Lett. Univ. Zilina* **19** (3), 77–82 (2017). <https://doi.org/10.26552/com.C.2017.3.77-82>
14. J.-L. Zhao, P. Zhang, J.-B. Zhou, D.-X. Yang, D.-S. Yang, and E.-P. Li, "Visualizations of light-induced refractive index changes in photorefractive crystals employing digital holography," *Chin. Phys. Lett.* **20**, 1748–1751 (2003). <https://doi.org/10.1088/0256-307X/20/10/327>
15. M. Fu, C. Gao, X. Wang, Y. Cui, and S. Dai, "A method for probing the refractive index change in photorefractive crystals," *Opt. Appl.* **43**, 731–737 (2013). <https://doi.org/10.5277/oa130409>
16. K. Peithmann, A. Wiebrock, K. Buse, and E. Krätzig, "Low-spatial-frequency refractive-index changes in iron-doped lithium niobate crystals upon illumination with a focused continuous-wave laser beam," *J. Opt. Soc. Am. B* **17**, 586–592 (2000). <https://doi.org/10.1364/JOSAB.17.000586>
17. A. D. Bezpaly, A. O. Verkhoturov, and V. M. Shandarov, "Optical writing of channel waveguides and 1D diffraction gratings in photorefractive surface layers of lithium niobate," *Ferroelectrics* **515**, 34–43 (2017). <https://doi.org/10.1080/00150193.2017.1360106>
18. A. D. Bezpaly, A. O. Verkhoturov, V. M. Shandarov, "Channel waveguides and phase diffraction gratings optically formed in photorefractive surface layers of lithium niobate," *Proc. SPIE* **10603**, 106030O (2017). <https://doi.org/10.1117/12.2292320>
19. A. D. Bezpaly, V. M. Shandarov, A. E. Mandel, V. I. Bykov, and K. M. Mambetova, "Optically induced channel waveguide structures with spatial modulation of parameters in the surface layer of lithium niobate," *Russ. Phys. J.* **62**, 387–392 (2019). <https://doi.org/10.1007/s11182-019-01724-w>
20. Yu. Jia and F. Chen, "Compact solid-state waveguide lasers operating in the pulsed regime: A review," *Chin. Opt. Lett.* **17**, 012302 (2019).
21. K. M. Mambetova, S. M. Shandarov, L. N. Orlikov, S. I. Arestov, S. V. Smirnov, L. Ya. Serebrennikov, and V. A. Krakovskii, "Formation of dynamic photorefractive gratings in a LiNbO₃:Cu surface-doped crystal," *Opt. Spectrosc.* **126**, 781–786 (2019). <https://doi.org/10.1134/S0030400X1906016X>
22. O. Althoff, A. Erdmann, L. Wiskott, and P. Hertel, "The photorefractive effect in LiNbO₃ at high light intensity," *Phys. Status Solidi A* **128**, K41–K46 (1991). <https://doi.org/10.1002/pssa.2211280138>
23. D. C. Ghiglia and L. A. Romero, "Robust two-dimensional weighted and unweighted phase unwrapping that uses fast transforms and iterative methods," *J. Opt. Soc. A* **11**, 107–117 (1994). <https://doi.org/10.1364/JOSAA.11.000107>
24. P. Günter and J.-P. Huignard, *Photorefractive Materials and Their Applications 2: Materials*, Springer Series in Optical Sciences (Springer, Berlin, 2007).
25. B. I. Sturman and V. M. Fridkin, *Photohalvanic Effect in Media without Central Symmetry and Related Phenomena* (Nauka, Moscow, 1992).

Translated by V. Arutyunyan